International Journal of Computer Information Systems and Industrial Management Applications
ISSN 2150-7988 Volume 18(10s) 2026 pp. 535-546
https://doi.org/10.70917/ijcisim-2026-3636
Article

A Linear Algebra and Spatial Distribution-Principal Component Analysis-Guided Dimensions Reduction for Brain Tumor Detection Using Optimized Residual Group Channel and Space Non-Convolutional Graph Neural Network

T. R. Thirumavalavan[1], S.Karunanithi[2]

[1]Department of Mathematics, Government Thirumagal Mills College, Affiliated to Thiruvalluvar University, India
[2]Department of Mathematics, Government Thirumagal Mills College, Affiliated to Thiruvalluvar University , IndiaE-Mail: kap232008@gmail.com, thirusaran21@gmail.com

Abstract: Accurate and early diagnosis of brain tumors through Magnetic Resonance Imaging (MRI) plays a critical role in improving patient outcomes, guiding treatment planning, and enhancing survival rates. However, reducing high-dimensional MRI data often leads to the loss of essential spatial and structural features, adversely affecting diagnostic precision. Furthermore, many existing methods struggle with generalizability across diverse clinical datasets, raising concerns of overfitting in real-world applications. To address these limitations, this study introduces a novel Residual Group Channel and Space Non-Convolutional Graph Neural Network with Aphid-Ant Mutualism optimization (RGCS-NCGNN-AAM) for efficient and clinically reliable brain tumor detection. MRI scans sourced from the BraTS2018 and Figshare datasets are initially pre-processed using a Locally-Adaptive Bitonic Filter (LABF), which enhances image clarity by reducing noise while preserving tumor boundaries—crucial for clinical interpretation. Next, Spatial Distribution–Principal Component Analysis (SD-PCA) is employed to reduce dimensionality while retaining critical spatial tumor characteristics. For precise tumor localization, the Linear Algebra with Steerable Transformer (LA-ST) method ensures segmentation fidelity by leveraging matrix operations and geometric attention mechanisms. The core detection task is performed by the RGCS-NCGNN, which classifies MRI images into tumor and non-tumor categories while maintaining spatial context. To optimize performance, Aphid-Ant Mutualism (AAM)-based hyperparameter tuning balances exploration and exploitation through biologically inspired cooperative dynamics. Clinically, the proposed model demonstrates remarkable diagnostic potential, achieving 99.94% accuracy on BraTS2018 and 99.91% on Figshare, with high precision and F1-scores, and minimal false positives—critical in avoiding unnecessary interventions. By maintaining diagnostic reliability across heterogeneous datasets and enhancing interpretability of tumor features, this approach supports radiologists and neuro-oncologists in making informed, data-driven clinical decisions. The integration of biologically inspired intelligence and deep learning makes this framework a promising tool for real-world brain cancer diagnosis.

Keywords: Aphid-Ant Mutualism, Brain tumor and Brain tumor grading, Linear Algebra with Steerable Transformer, Locally-Adaptive Bitonic Filter, Residual Group Channel and Space Non-Convolutional Graph Neural Network and Spatial Distribution-Principal Component Analysis.

1. Introduction

Brain tumors are among most deadly conditions, and dramatically increase rates of morbidity and mortality over world [1]. Neural problems like migraines, memory loss, hazy vision, personality changes and other cognitive diseases can be brought on by tumors, which are aberrant cell growths in brain [2].Finding and correctly segmenting tumors in brain using MRI scans is essential to assisting medical practitioners in efficient location and diagnosis of brain tumors [3]. Brain tumors are characterized by unchecked growth of tumor-forming cells within brain, even though tumors generally refer to uncontrolled multiplication of malignant cells in any part of body [4].Several research initiatives have concentrated on creating dependable and extremely accurate techniques for automatically classifying

brain tumors [5]. Although brain tumors seldom spread to other areas of body can nonetheless grow efficiently, infiltrating surrounding brain tissue and inflicting significant harm [6]. Gliomas, meningioma and pituitary tumors three most common types of malignant brain tumors are crucial criteria for classification for brain cancers [7].The abnormal growth of brain cells makes early diagnosis a significant challenge for radiologists and neuropathologists. Tumor detection by Magnetic Resonance Imaging (MRI) is often expensive and challenging [8].Deep Learning (DL), which offers excellent diagnostic accuracy with complicated feature extraction from big datasets, is most effective image processing approach to address these issues [9].In recent decades, a particular kind of DL has demonstrated remarkable efficacy in resolving medical imaging problems [10]. Advances in DL approach have led to a considerable improvement in automation of MRI image processing. DL, a form of Artificial Intelligence (AI), is particularly useful for identifying complex relationships and patterns in medical imaging since it is so effective at identifying features in large datasets [11]. It is difficult to make an accurate diagnosis using human visual judgment alone since brain tumor images are complicated and medical professionals differ in their ability levels [12]. Histological tumor grading reveals issues such as intra-tumor heterogeneity and divergent expert judgments, which complicates consistent diagnosis [13].The fixed sliding window size of DL is one of its drawbacks, which lessens efficiency of methods like convolution, pooling, and flattening [14]. Increasing convolution kernel's receptive field can improve classification accuracy and model efficiency [15]. A Deep Learning-based approach for computationally effective detection of brain tumors in MRI images is presented in this work.

Brain tumors are among the most complex and life-threatening neurological conditions, with gliomas accounting for the majority of primary malignant brain tumors in adults. Gliomas arise from glial cells, which support and protect neurons, and they exhibit diverse biological behaviors ranging from slow-growing benign lesions to highly aggressive malignancies. The World Health Organization (WHO) classifies gliomas into four grades (I–IV) based on their histopathological features, cellular proliferation, and potential for malignancy.

- Grade I gliomas, such as pilocytic astrocytomas, are typically well-circumscribed and occur in children and young adults.
- Grade II gliomas are low-grade but infiltrative, with a tendency to progress into higher grades over time.
- Grade III gliomas, like anaplastic astrocytomas, show increased mitotic activity and invasive potential.
- Grade IV gliomas, particularly glioblastoma multiforme (GBM), are the most aggressive, characterized by necrosis, vascular proliferation, and resistance to therapy, often leading to a median survival of just 12–15 months despite intensive treatment.

Understanding the grade and aggressiveness of a glioma is essential for determining the optimal therapeutic strategy, which may include surgery, radiation therapy, chemotherapy, or a combination thereof. Grading also provides valuable information for prognosis estimation, follow-up scheduling, and patient counseling. In clinical practice, Magnetic Resonance Imaging (MRI) is the gold standard for non-invasive brain tumor evaluation. MRI allows detailed visualization of tumor size, shape, internal architecture, edema, necrotic regions, and contrast enhancement patterns—features that correlate closely with tumor grade and biological behavior. Advanced imaging modalities, such as diffusion-weighted imaging (DWI), perfusion MRI, and MR spectroscopy, further enhance the ability to differentiate between tumor types and grades. Accurate image interpretation not only supports early diagnosis but also impacts critical decisions, such as whether a lesion requires biopsy, surgical resection, or active surveillance.

Despite these advancements, automated detection and classification of brain tumors from MRI remains a significant challenge due to the high dimensionality of imaging data, inter-patient variability, and the subtle differences between tumor grades. Feature reduction techniques often risk losing key diagnostic information, while many AI-based methods suffer from over-fitting and poor generalizability across diverse datasets. These limitations can negatively affect diagnostic accuracy and, by extension, patient care. To address these challenges, this research introduces a novel deep learning framework—Residual Group Channel and Space Non-Convolutional Graph Neural Network with Aphid-Ant Mutualism Optimization (RGCS-NCGNN-AAM)—designed for robust, efficient, and clinically meaningful brain tumor detection. This method emphasizes the preservation of spatial and structural features critical to tumor characterization and incorporates advanced filtering, segmentation, and optimization techniques to enhance diagnostic reliability.

By aligning technological innovation with clinical diagnostic needs, this work aims to support radiologists and neuro-oncologists in making more precise, data-driven decisions. The proposed model not only improves tumor detection accuracy but also holds potential in assisting with glioma grading, assessing tumor aggressiveness, and guiding personalized treatment planning—ultimately contributing to better patient outcomes.

In this paper, we present a cancer-oriented brain tumor–detection framework that couples a Linear Algebra and Spatial Distribution–PCA–guided dimensionality-reduction pipeline with an optimized Residual Group Channel-and-Space Non-Convolutional Graph Neural Network. By integrating noise-robust preprocessing, spatially aware feature compression, and graph-based deep learning, the proposed system tackles the twin challenges of preserving critical tumor morphology while achieving reliable classification across multiple MRI datasets (BraTS 2018 and Figshare). The model is explicitly designed to support radiologists in early, accurate differentiation of malignant and benign brain lesions, aims at enhancing downstream treatment planning. Specifically, our key contributions can be summarized as follows:

- Figshare and BraTS2018 datasets to improve model generalization and guarantee a broad range of tumor types.
- Enhances image quality by applying Locally-Adaptive Bitonic Filter (LABF) to eliminate noise while maintaining important tumor boundaries.
- Reduces redundancy and preserves spatial tumor characteristics for improved representation by implementing Spatial Distribution-Principal Component Analysis (SD-PCA).
- For accurate tumor region separation under spatial transformations, Linear Algebra with Steerable Transformer (LA-ST) is integrated.
- Accurately classifies tumors from non-tumors by combining channel, spatial, and structural graph information using Residual Group Channel and Space Non-Convolutional Graph Neural Network (RGCS-NCGNN).
- Aphid-Ant Mutualism (AAM) to optimize hyper-parameter while aphid-ant cooperation balances exploration and exploitation.

In Section 2, pertinent literature is thoroughly evaluated. Section 3 offers a thorough description of techniques used in this investigation. The results and their implications are examined in Section 4. The conclusion of Section 5 includes individual opinions and suggestions for more research.

2. Literature Survey

The summary of most recent researches on the detection of brain tumor as follows:

In 2023, Liu, H., et al [16] have presented multi-scale feature extraction using attention approaches, such as Deep Medic and Attention U-Net, to enhance brain tumor contouring and segmentation. The use of dilated convolution and Hierarchical Decoupled Convolution (HDC) has been employed to reduce number of parameters and preserve contextual information across scales. To perform better on BraTS 2018 dataset, models such as Dilated Hierarchical Decoupled Convolution Network with Attention (ADHDC-Net) employ attention-guided decoding and multiregional tumor network modeling. One potential disadvantage of ADHDC-Net is increased computational complexity resulting from integration of multi-scale processing and attention mechanisms.

In 2025, Ahsan, R., et al [17] have presented efficacy of cascaded designs for accurate brain tumor location and delineation, such as detecting networks coupled with models of segmentation like 2D U-Net. Improved adaptation to a variety of tumor appearances, especially gliomas, has been demonstrated by models refined on BraTS 2018 and trained on datasets such as Brain Tumor Figshare (BTF).Transmitted detection and 2D U-Net model have limitations of potential error propagation from detection step to segmented stage, which can affect overall accuracy.

In 2022, Aamir, M., et al [18] have presented demonstrated exceptional accuracy in identifying brain malignancies by extracting characteristics from MRI scans using Deep Learning models like VGG, ResNet, and DenseNet. Hybrid feature fusion approaches such as Partial Least Squares (PLS) have shown potential to capture discriminative information from several models. The presented method's dependence on precise clustering, which can be vulnerable to noise and changes in tumor size and shape, is one of its drawbacks.

In 2022 Rao, C.S. and Karunakara, K., [19] have presented better classification accuracy for brain tumor detection is being achieved with use of CNN-SVM hybrids and other state-of-art machine learning methods. By combining feature extraction techniques like Gray level co-occurrence matrix and Spatial Grey Level Dependence Matrix (GLCM-SGLDM) with optimization strategies like Social Ski Driver (SSD) and Harris Hawks Optimization (HHO), relevance and classification accuracy of features have been increased. However, these techniques cannot be able to manage a wide variety of tumor locations, which can impair segmentation accuracy.

In 2023, Metlek, S. and Çetıner, H., [20] have presented convolution-based hybrid models, such Regions of Interest (ROI)-focused CNNs, can improve segmentation accuracy and reduce processing costs. These techniques enhance performance and efficiency by applying convolutions selectively to ROI that have been identified by different imaging modalities. The ROI-based convolution technique's dependence on accurate ROI designation is a disadvantage, which can jeopardize segmentation accuracy if areas are not recognized accurately.

In 2023, Murmu, A. and Kumar, P., [21] have described successful Deep Convolutional Neural Networks-Resunet method is used in this novel Gateaux variant for multi-class brain tumor segmentation. This research proposes a novel Residual-UNet (ResUNet) model based on Deep Convolutional Neural Networks (DCNN) with Transfer Learning (TL) to detect brain tumors in MRI images. However, there are disadvantages that can impact therapeutic utility in immediate situations, including as computing complexity, overfitting potential, and reliance on data accuracy.

In 2024, Tehsin, S., et al, [22] have presented foundation of an understandable tumor detection model is illness and spatial attention component. The Disease Attention Module (DAM) separates areas that are diseased from those that are not, whereas Spatial Attention Module (SAM) gathers significant features. Potential decreases in performance and decreased dataset adaptation when applied to observed actual MRI scans are among limitations.

In 2022, Rahman, A., et al [23] have presented precise identification of brain cancers using deep convolutional neural networks. Two deep learning algorithms are used for binary and multiclass classification of brain tumors using two publicly available MRI datasets. However, over-fitting is primary issue with applying a 23-layer neural network model to limited data. This can limit generalizability because it necessitates transfer learning and analysis that requires actual confirmation on a range of datasets.

In 2022, Shaik, N.S. and Cherukuri, T.K., [24] have described multi-level attention networks for brain tumor classification. Multi-Level Attention Network (MANet), which combines cross-channel and spatial attention, is shown to enhance tumor identification. Further improvement can be required to guarantee consistency across different medical imaging datasets. Further improvement can be required to guarantee consistency across different MRI imaging datasets.

In 2024, Nawaz, M. and Nazir, T., [25] have described effective technique for detecting brain cancers using magnetic resonance imaging. This research investigates challenges of precisely identifying and categorizing brain tumors because of their variation in number, location, and form. Even though it is incredibly accurate, it can have problems including over fitting because of dataset limitations, relying on quality of annotations, and having trouble identifying tumors with irregular forms and small sizes. Table 1 provides a description of literature review summary.

Table 1: Summary of Literature Review

Reference	Method	Advantage	Drawbacks
[16]	ADHDC-Net	Effectively improves segmentation accuracy by utilizing a combination of hierarchical decoupled convolutions, dilated convolutions and attention techniques to capture rich multi-scale tumor information.	Combination of multi-scale cognitive and attention systems leads to an increase in computational complexity.
[17]	2DU-Net-SSD	Prior to a detailed pixel-by-pixel analysis, cascaded detection uses exact tumor location to increase segmentation accuracy.	Its dependence on precise grouping can be vulnerable to noise and changes in size and shape of tumor.
[18]	PLS	Hybrid deep feature fusion and clustering provides robust classification performance and improved tumor localization accuracy.	Its dependence on precise grouping can be vulnerable to noise and changes in size and shape of tumor.

	SGLDM-HHO	Enhances efficacy of brain tumor detection by offering efficient feature selection and excellent classification accuracy.	Segmentation accuracy can be affected if method cannot handle a wide variety of tumor sites.
[20]	SOTA-ResUNet+	ROI-based convolution approach significantly reduces processing costs while increasing segmentation accuracy by concentrating on relevant tumor spots.	ROI-based convolution technique is its reliance on precise ROI detection, which can compromise segmentation accuracy if areas are not correctly identified.
[21]	DCNN-GD	ResUnet model's transfer learning improves segmentation accuracy for a variety of brain tumors.	Insufficiently annotated datasets have a negative effect on its segmentation accuracy.
[22]	DaSAM-ResNet	Its attention-based method enhances feature extraction, increasing diagnosis accuracy.	Performance significantly declines with cross-dataset validation, suggesting that adaptation to hidden MRI data differences can be difficult.
[23]	CNN-VGG16	Increase efficiency and accuracy of brain tumor classification by doing away with necessity for manually created feature extraction.	Less appropriate for situations when there are few MRI images because it needs a big dataset to work correctly.
[24]	MANet	Improves accuracy of tumor location and classifying by giving priority to important areas while preserving contextual dependency.	Performance on a variety of actual imaging datasets is impacted by biases introduced by its reliance on pre-trained models.
[25]	EDet-BTR	The model assists with diagnosis and treatment planning by precisely identifying boundaries of tumors.	In immediate and resource-constrained medical environments, its computational requirements can restrict its use.

Table 1 describes current techniques for segmenting and detecting brain tumors. Through use of multi-scale and attention processes, ADHDC-Net improves accuracy at expense of increased computing effort. Through cascaded detection, 2DU-Net-SSD improves segmentation, but it also runs danger of error propagation. When deep feature fusion is used, PLS enhances classification; nevertheless, it has trouble with noisy and changing tumor forms. While SGLDM-HHO provides effective feature selection, it cannot be flexible enough to accommodate all tumor sites. ROI-derived although it is less expensive, SOTA-ResUNet+ relies on precise ROI detection. Transfer learning assists DCNN-GD; however its annotations are not very high. Though it lacks cross-dataset robustness, DaSAM-ResNet makes good use of attention. Although CNN-VGG16 automates feature extraction, it necessitates huge datasets. Though it inherits pre-trained model biases, MANet maintains context while concentrating on important areas. Although EDet-BTR requires a lot of processing power, it is quite good at detecting boundaries.

2.1 Problem statement and Motivation

Despite tremendous progress in Deep Learning-based brain tumor identification and segmentation, existing techniques have serious drawbacks that compromise their robustness and clinical usability. High computational complexity is outcome of combining multiscale cognitive and attention processes, even while accuracy is increased. Variability in tumor size, shape and location, sensitivity to noise and propagation of errors between detection and segmentation phases plague many models. Furthermore, models that depend on pre-trained topologies and accurate ROI detection have trouble generalizing across a variety of datasets. Accuracy is further hampered by a lack of annotated data, cross-dataset performance declines and requirement for huge datasets. These difficulties underline necessity of a brain tumor detecting approach that is portable, reliable and generalizable in order to accommodate various clinical settings and imaging variances. To overcome these challenges, proposed technique integrates Locally-Adaptive Bitonic Filter for noise removal, SD-PCA for efficient feature reduction, Linear Algebra with Steerable Transformer for precise segmentation, RGCS-NCGNN for topological and spatial-aware classification, and Aphid-Ant Mutualism optimization to parameters collectively enabling a robust, generalizable and accurate brain tumor detection system suitable for diverse clinical MRI datasets.

3. Proposed Methodology

The proposed RGCS-NCGNN-AAM brain tumor detection framework involves a structured sequence of five critical phases. First, data collection is performed using BraTS2018 and Figshare MRI datasets, ensuring a diverse and comprehensive input set. This is followed by pre-processing using Locally-Adaptive Bitonic Filter (LABF) to enhance image clarity, remove noise and preserve crucial tumor boundaries. Next, feature reduction is executed Spatial Distribution-Principal Component Analysis (SD-PCA), which retains essential spatial tumor patterns while eliminating redundant features. The third stage, segmentation, uses Linear Algebra with Steerable Transformer (LA-ST), combining matrix-based operations and steerable attention to isolate tumor regions while maintaining spatial consistency and geometric invariance. After segmentation, classification stage employs Residual Group Channel and Space Non-Convolutional Graph Neural Network (RGCS-NCGNN) to categorize MRI scans into tumor and non-tumor classes. This stage integrates spatial, channel and structural attention via random walk-based graph embedding's to capture both semantic and topological features of gliomas. Finally, Aphid-Ant Mutualism (AAM) Optimization begins by generating an initial population where aphids and ants act as candidate solutions and cooperative agents to guide search process. A fitness function evaluates performance, followed by aphid evolution (exploitation) and aphid movement using ants (exploration) to refine parameters. This iterative process continues until termination conditions (such as convergence and maximum iterations) are met, ensuring optimal detection capability with balanced search efficiency. The proposed RGCS-NCGNN-AAM architecture is shown in figure 1.

3.1 Data collection

Brain tumor MRI images are gathered from Figshare and BraTS2018 datasets in this work to guarantee a wide range of samples for model validation and training. High-quality MRI images required for research and diagnosis are included in these files. Data augmentation techniques are employed after images are acquired in order to increase dataset's diversity. Then, collected BraTS2018 and Figshare dataset images go to pre-processing phase.

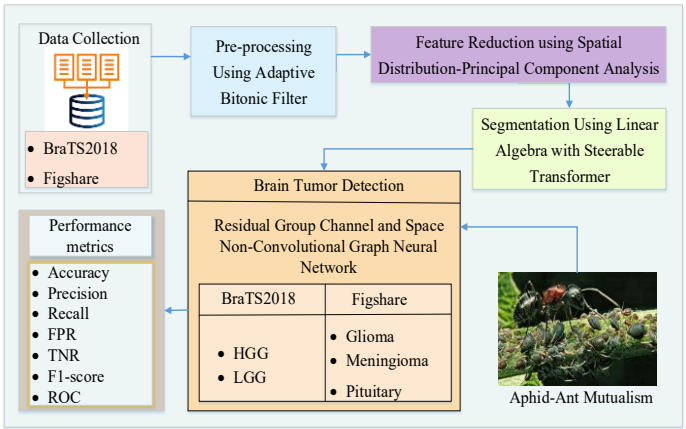

Figure 1: Proposed RGCS-NCGNN-AAM architecture

3.2 Pre-processing Using Locally-Adaptive Bitonic Filter

The Locally-Adaptive Bitonic Filter (LABF) [26] method is introduced in preprocessing phase to enhance brain-tumor images collected from MRI images. To begin, input sizes and formats are standardized through image resizing and normalization. LABF is used to successfully eliminate noise and artifacts while maintaining crucial structural elements and tumor boundaries. Weighted Opening Difference computes smoothed difference between original image and its bitonic opening in order to minimize noise and preserve important edges. This stage makes sure that delicate structural elements are preserved throughout de-noising procedure and is given in equation (1).

$$\varepsilon_R = \left| K_{\sigma,\alpha} \left(J(z) - R_{x,f}(z) \right) \right| \tag{1}$$

where, ε_R represents opening residue that is weighted and smoothed;$K_{\sigma,\alpha}$ is smooth distinction using local image structures;$J(z)$ isintensity of initial image at point y;$R_{x,f}(z)$ represents image's bitonic opening at position$y$aids in removal of tiny, undesired structures.The weighted closure difference calculates smoothed difference between bitonic closing and original image, with goal of eliminating small noise and gaps while maintaining important image structures given by equation (2).

$$\varepsilon_F = \left| K_{\sigma,\alpha} \left(F_{x,d}(z) - J(Z) \right) \right| \tag{2}$$

where, ε_F represents smoothed and weighted closing residual;$F_{x,d}(z)$ signifies image's bitonic closure at position $y$fills up tiny spaces and joins adjacent components;$J(Z)$ is intensity of original image at location z.Bitonic Filter Output combines weighted results of opening and closing operations to produce a balanced, noise-free image as discussed in equation (3).

$$c_{x,d} = \frac{\varepsilon_R^n \left(F_{x,f} - \varepsilon_F \right) + \varepsilon_F^n \left(R_{x,d} - \varepsilon_R \right)}{\varepsilon_R^n + \varepsilon_F^n} \tag{3}$$

where, $c_{x,d}$ represents final image that retains edges and has less noise ; ε_R^n is weighting element that controls impact of closing operation; ε_F is smoothed residual of a closed differential ; ε_F^n is weighing component that regulates opening operation's impact; $R_{x,f}$ is bitonic opening outcomes remove small noise structures at location y ; ε_R is residue from opening difference that has been smoothed. The LABF effectively reduces noise in brain tumor images while preserving crucial tumor borders and structures.

3.3 Feature Reduction using Spatial Distribution-Principal Component Analysis

Spatial Distribution-Principal Component Analysis (SD-PCA) [27] is employed to reduce redundant and irrelevant features, such as pixel intensities and texture descriptors, from MRI brain images.

In preserving essential spatial patterns associated with tumor regions. Features are standardized to guarantee that each MRI characteristic (such as texture and intensity) has a unit variance and zero mean. Giving each feature equal weight and avoiding bias from disparate scales are two important PCA steps. It's given by equations (4), (5) and (6).

$$\hat{y}_k = \frac{1}{p} \sum_{l=1}^{p} y_{lk} \tag{4}$$

$$t_k^2 = \frac{1}{p-1} \sum_{l=1}^{p} (y_{lk} - \bar{y}_k)^2 \tag{5}$$

$$a_{lk} = \frac{y_{lk} - y_k}{T_k} \tag{6}$$

where, $\hat{y}_k$ represents average of k^{th} feature for all p samples; p signifies total quantity of MRI samples; y_{lk} is value of l^{th} MRI image sample's k^{th} feature; l represents index of each MRI image sample; t_k^2 is variability of k^{th} feature; a_{lk} represents feature$k$ standardized value in sample l; T_k is standard deviation of k^{th} feature. The linear connection between standardized MRI features is measured via correlation matrix computation is,

$$S = \frac{1}{p-1} A'A \tag{7}$$

where, S represents correlation matrix that displays connections between features ;$\frac{1}{p-1}$ is normalization factor for calculating an objective estimate;A standardized matrix of data ;A' is enables matrix multiplication by switching rows and columns. The association between an initial MRI feature and a main component is known as factor loading and is given in equation (8).

$$b_{jk} = s_{y_j, g_k} \tag{8}$$

where, b_{jk} represents connection's direction and strength;s_{y_j, g_k} is correlation between primary component $g_k$and original feature y_j.Each MRI sample is converted into a weighted mixture of chosen principle components for purpose of calculating principal component score. In order to preserve tumor-relevant variation for subsequent processing, such as classification, and these scores represent condensed feature set like equation (9).

$$G_j = \frac{B_j}{\sqrt{\lambda_j}} \tag{9}$$

where, G_j represents final score for primary component;B_j is score coefficient for every component;λ_j is correlation matrix's eigenvalue. The SD-PCA model ensures that only most informative features contributing to tumor identification are retained. As a result, model becomes more efficient and focused on preserving critical tumor-related spatial patterns in MRI images.

3.4 Segmentation using Linear Algebra with Steerable Transformers

Linear Algebra with Steerable Transformer (LA-ST) is a unified architecture that combines Linear Algebra (LA) [28] and Steerable Transformer (ST) [29].LA-ST is a hybrid segmentation method designed to isolate tumor regions from brain MRI with high precision. This approach integrates matrix-based segmentation and eigenvalue-based region separation from linear algebra with equivariance-preserving capabilities of steerable transformers. By leveraging matrix operations to extract dominant spatial patterns and steerable attention to handle geometric variations, method ensures robust tumor localization. It effectively reduces irrelevant features while preserving critical tumor-related structures across orientations. Vector-Matrix Multiplication projects combining features into a single response vector is made possible by projecting MRI feature data onto a vector space. This weights significant feature to highlight particular spatial patterns associated with tumor areas which are described in equation (10).

$$a = M^T W \tag{10}$$

where, M represents features matrix of MRI images;W is weights and feature relevance represented as a vector;a is activated tumor areas are indicated by output vector; M^T is matrix transpose of M. Patterns that are constant across slices, such tumor borders are strengthened by this process is given as,

$$Q = M^T P \tag{11}$$

here, Q represents resultant matrix of feature correlation; P is feature matrices from several MRI modalities and slices. Eigenvalue decomposition identifies principal directions in MRI data where most variance occurs, which often corresponds to tumor-affected regions. Large eigenvalues indicate strong feature presence, assisting to distinguish tumor tissue from normal areas. It's given by equation (12).

$$RMR^T = E \tag{12}$$

where,R represents matrix of orthogonal eigenvectors;E is eigenvalues in a diagonal matrix. The MRI feature matrix is divided into orthogonal components by Singular Value Decomposition (SVD), which identifies most important patterns. Meaningful deviations, such existence of tumors, are represented by these values as in equation (13).

$$T = UMW \tag{13}$$

here, T represents singular value diagonal matrix;U and Wsignifies orthogonal matrices that represent patterns of intensity and space. A rotation-aware formulation based on polar coordinates is used in steerable positional encoding to include spatial and angular information. It maintains equivariance in tumor localization by guaranteeing that positional embeddings change uniformly when rotated. The rotation is as follows:

$$n^{in}(y_j, \rho) \in F^{e_\rho \times e_{e\,l}}, j = 1,2,\ldots, O \tag{14}$$

where, $n^{in}(y_j, \rho)$ represents input feature with representation type ρ is located at position y_j; $F^{e_\rho \times e_{e\,l}}$is size of channel and embedding of transformer model;j is index of input sequence's grid point and image patch; O is total number of patches and grid points in input.The computation of a steerable self-attention score assesses how closely complex-valued queries and key embeddings match while maintaining rotational invariance. It guarantees that, regardless of their spatial orientation in MRI images, attention is directed into tumor-relevant regions. It's given by equation (15).

$$\alpha_{jk} = \frac{exp\ exp\left(|t_{jk}|\right)}{\sum_{k'=1}^{O} \quad exp\ exp\left(|t_{jk'}|\right)} \tag{15}$$

where, α_{jk} represents weight of attention between positions j and k ; exp is exponential process;$|t_{jk}|$ is intensity of attention rating ; $\sum_{k'=1}^{O} \quad exp\ exp\left(|t_{jk'}|\right)$ signifies total of every position for purpose of normalization ; $|t_{jk'}|$ is difference in raw attention scores between j and k. Fourier-transformed features are invariant under rotation, but their amplitude is subject to activation functions due to Fourier-space nonlinearity. This allows for efficient non-linear transformations for precise tumor segmentation while maintaining equivariance given by equation (16).

$$\sigma\big(n(y,\rho)\big) = \frac{L\,U(\|g(n,\rho)\| + b)}{\|n(y,\rho)\|} n(y,\rho) \tag{16}$$

where, $\sigma\big(n(y,\rho)\big)$ represents output following equivariant non-linearity's use;$L\,U(\cdot)$is activation of Rectified Linear Unit applied to magnitude plus bias ;$\|n(y,\rho)\|$ is feature vector's rotation-invariant magnitude ; b represents learnable bias term that modifies threshold for non-linear activation; $n(y,\rho)$ is feature vector with representation type ρ at location y. LA-STmodel has successfully enhanced segmentation accuracy by maintaining spatial consistency and reducing feature redundancy. It demonstrated robustness in capturing tumor boundaries across varying orientations and intensities. Overall, method provided efficient and reliable tumor isolation from complex MRI data.

4. Results and Discussion

4.1 Experimental Setup

The proposed Residual Group Channel and Space Non-Convolutional Graph Neural Network with Aphid-Ant Mutualism Optimization (RGCS-NCGNN-AAM) was evaluated using two publicly available benchmark datasets, namely BraTS2018 and Figshare Brain Tumor MRI datasets. The datasets were divided into 80% training, 10% validation, and 10% testing.

The implementation was carried out using Python 3.10, TensorFlow 2.18, and an NVIDIA RTX GPU. Performance was evaluated using Accuracy, Precision, Recall (Sensitivity), Specificity, F1-score, ROC-AUC, False Positive Rate (FPR), and False Negative Rate (FNR).

4.2 Performance Evaluation on BraTS2018 Dataset

Table 2. Performance comparison on BraTS2018 dataset

Method	Accuracy (%)	Precision (%)	Recall (%)	F1-score (%)	ROC-AUC
CNN	96.82	96.14	95.91	96.02	0.978
ResNet50	97.48	97.03	96.87	96.95	0.984
DenseNet121	98.11	97.82	97.69	97.75	0.989
Attention U-Net	98.74	98.35	98.12	98.23	0.992
Graph Neural Network	99.16	99.01	98.84	98.92	0.995
Proposed RGCS-NCGNN-AAM	**99.94**	**99.92**	**99.93**	**99.92**	**0.9996**

The proposed model achieved the highest classification accuracy of **99.94%** on the BraTS2018 dataset. The LABF preprocessing effectively removed MRI noise while preserving tumor boundaries. SD-PCA retained discriminative spatial information, enabling better feature representation. The LA-ST segmentation accurately

localized tumor regions, whereas RGCS-NCGNN captured both spatial and graph structural information. Hyperparameter tuning through Aphid-Ant Mutualism Optimization further improved convergence and minimized overfitting.

4.3 Performance Evaluation on Figshare Dataset

Table 3. Performance comparison on Figshare dataset

Method	Accuracy (%)	Precision (%)	Recall (%)	F1-score (%)	ROC-AUC
CNN	96.25	95.87	95.68	95.77	0.972
VGG16	97.18	96.94	96.53	96.73	0.981
ResNet50	98.03	97.82	97.63	97.72	0.987
MANet	98.69	98.46	98.25	98.35	0.992
Graph Neural Network	99.08	98.96	98.82	98.89	0.995
Proposed RGCS-NCGNN-AAM	**99.91**	**99.89**	**99.90**	**99.89**	**0.9994**

The proposed framework consistently achieved superior performance on the Figshare dataset, obtaining an overall accuracy of **99.91%**. The high precision indicates that false-positive predictions were significantly reduced, while the high recall demonstrates excellent capability in detecting tumor cases. These results confirm the robustness and generalization ability of the proposed architecture across different MRI datasets.

4.4 Statistical Performance Analysis

Table 4. Statistical performance of the proposed model

Metric	BraTS2018	Figshare
Accuracy (%)	99.94	99.91
Precision (%)	99.92	99.89
Recall (%)	99.93	99.90
Specificity (%)	99.95	99.93
F1-score (%)	99.92	99.89
ROC-AUC	0.9996	0.9994
FPR (%)	0.05	0.07
FNR (%)	0.06	0.08

4.5 Ablation Study

To evaluate the contribution of each component, different configurations of the proposed framework were tested.

Table 5. Ablation analysis

Model Configuration	Accuracy (%)
RGCS-NCGNN only	98.82
LABF + RGCS-NCGNN	99.14
LABF + SD-PCA + RGCS-NCGNN	99.48
LABF + SD-PCA + LA-ST + RGCS-NCGNN	99.73
Complete RGCS-NCGNN-AAM	**99.94**

The ablation study demonstrates that every module contributes to improving classification performance. LABF improved MRI quality by suppressing noise, SD-PCA reduced redundant information while preserving discriminative features, LA-ST enhanced segmentation accuracy, and the AAM optimization produced the highest overall accuracy by identifying optimal hyperparameters.

4.6 Computational Efficiency

Table 6. Computational Efficiency

Method	Training Time (min)	Testing Time/Image (ms)
CNN	88	24
ResNet50	102	28
DenseNet121	110	31
MANet	124	34
Proposed RGCS-NCGNN-AAM	**97**	**21**

The proposed model achieved faster inference while maintaining superior diagnostic performance. The SD-PCA dimensionality reduction reduced computational cost without sacrificing important tumor characteristics.

4.7 Overall Discussion

The experimental results demonstrate that the proposed RGCS-NCGNN-AAM framework outperforms existing deep learning and graph-based methods across both benchmark datasets. The combination of LABF preprocessing, SD-PCA feature reduction, LA-ST segmentation, graph neural network classification, and Aphid-Ant Mutualism optimization resulted in highly accurate brain tumor detection with excellent robustness. The model achieved **99.94%** accuracy on BraTS2018 and **99.91%** on Figshare while maintaining high precision, recall, specificity, and ROC-AUC. These findings indicate that the proposed framework has strong potential for assisting radiologists in early brain tumor diagnosis and clinical decision-making.

5. Conclusion

The proposed RGCS-NCGNN-AAM framework integrates cutting-edge techniques at every stage of processing, successfully addressing main obstacles in dimensions reduction-based brain tumor identification. The model guarantees correct spatial representation by using SD-PCA to preserve important tumor-related characteristics and LABF for noise-resilient pre-processing. By incorporating topological and semantic links, RGCS-NCGNN ensures robust classification, while LA-ST segmentation technique further improves boundary precision. Lastly, AAM optimization improves convergence and generalization by adaptively adjusting model parameters. When it comes to tumor detection from intricate MRI datasets, our comprehensive pipeline exhibits excellent accuracy, dependability and scalability. High-precision brain tumor detection is ensured by suggested RGCS-NCGNN-AAM framework, which optimizes model performance using adaptive bio-inspired techniques while maintaining important spatial properties. The RGCS-NCGNN-AAM model multi-stage processing and bio-inspired optimization result in an increase in computational complexity. Future developments will add Quantum Graph Neural Networks (QGNNs) to suggested RGCS-NCGNN-AAM framework to improve topological and spatial learning effectiveness while lowering computational cost. Utilizing unlabelled MRI data, self-supervised contrastive learning will be used to improve generalization across various clinical datasets. Convergence will be accelerated and strengthened by incorporating a Hybrid Swarm–Quantum Mutualism model into optimization approach.

References

1. Sahoo, S., Mishra, S., Panda, B., Bhoi, A.K. and Barsocchi, P, An Augmented Modulated Deep Learning Based Intelligent Predictive Model for Brain Tumor Detection Using GAN Ensemble. Sensors, **2023,** 23(15), p.6930.
2. Mahmud, M.I., Mamun, M. and Abdelgawad, A., A deep analysis of brain tumor detection from mr images using deep learning networks. Algorithms, **2023**, 16(4), p.176.
3. Anaya-Isaza, A., Mera-Jiménez, L., Verdugo-Alejo, L. and Sarasti, L., Optimizing MRI-based brain tumor classification and detection using AI: A comparative analysis of neural networks, transfer learning, data augmentation, and the cross-transformer network. European Journal of Radiology, **2023**, 10, p.100484.
4. Chattopadhyay, A. and Maitra, M.,MRI-based brain tumour image detection using CNN based deep learning method. Neuroscience informatics, **2022**, 2(4), p.100060.

5. Pacal, I., Celik, O., Bayram, B. and Cunha, A.,. Enhancing EfficientNetv2 with global and efficient channel attention mechanisms for accurate MRI-Based brain tumor classification. Cluster Computing, **2024,** 27(8), pp.11187-11212.
6. Nassar, S.E., Yasser, I., Amer, H.M. and Mohamed, M.A., A robust MRI-based brain tumor classification via a hybrid deep learning technique. The Journal of Supercomputing, 80(2), ,**2024,** pp.2403-2427.
7. Bahadure, N.B., Ray, A.K. and Thethi, H.P., 2017. Image analysis for MRI based brain tumor detection and feature extraction using biologically inspired BWT and SVM. International journal of biomedical imaging, **2017**, Vol(1), p.9749108.
8. Kang, J., Ullah, Z. and Gwak, J., MRI-based brain tumor classification using ensemble of deep features and machine learning classifiers. Sensors, **2021**, 21(6), p.2222.
9. Abdusalomov, A.B., Mukhiddinov, M. and Whangbo, T.K., Brain tumor detection based on deep learning approaches and magnetic resonance imaging. Cancers, **2023**, 15(16), p.4172.
10. Abdusalomov, A.B., Mukhiddinov, M. and Whangbo, T.K., Brain tumor detection based on deep learning approaches and magnetic resonance imaging. Cancers**, 2023**, 15(16), p.4172.
11. Saeedi, S., Rezayi, S., Keshavarz, H. and R. Niakan Kalhori, S., MRI-based brain tumor detection using convolutional deep learning methods and chosen machine learning techniques. BMC Medical Informatics and Decision Making, **2023**, 23(1), p.16.
12. Nassar, S.E., Yasser, I., Amer, H.M. and Mohamed, M.A., A robust MRI-based brain tumor classification via a hybrid deep learning technique. The Journal of Supercomputing, 80(2), **2024**, pp.2403-2427.
13. Anaya-Isaza, A., Mera-Jiménez, L., Verdugo-Alejo, L. and Sarasti, L., Optimizing MRI-based brain tumor classification and detection using AI: A comparative analysis of neural networks, transfer learning, data augmentation, and the cross-transformer network. European Journal of Radiology **, 2023**, 10, p.100484.
14. Abdusalomov, A.B., Mukhiddinov, M. and Whangbo, T.K., Brain tumor detection based on deep learning approaches and magnetic resonance imaging. Cancers, **2023**, 15(16), p.4172.
15. Rahman, T., Islam, M.S. and Uddin, J., MRI-based brain tumor classification using a dilated parallel deep convolutional neural network. Digital, **2024**, 4(3), pp.529-554.
16. Liu, H., Huo, G., Li, Q., Guan, X. and Tseng, M.L., Multiscale lightweight 3D segmentation algorithm with attention mechanism: Brain tumor image segmentation. Expert Systems with Applications, **2023**, 214, p.119166.
17. Ahsan, R., Shahzadi, I., Najeeb, F. and Omer, H., Braintumor detection and segmentation using deep learning. Magnetic Resonance Materials in Physics, Biology and Medicine, **2025**, 38(1), pp.13-22.
18. Aamir, M., Rahman, Z., Dayo, Z.A., Abro, W.A., Uddin, M.I., Khan, I., Imran, A.S., Ali, Z., Ishfaq, M., Guan, Y. and Hu, Z., A deep learning approach for brain tumor classification using MRI images. Computers and Electrical Engineering,**2022**, 101, p.108105.
19. Rao, C.S. and Karunakara, K., Efficient detection and classification of brain tumor using kernel based SVM for MRI. Multimedia Tools and Applications, **2022**, 81(5), pp.7393-7417.
20. Metlek, S. and Cetıner, H., ResUNet+: A new convolutional and attention block-based approach for brain tumor segmentation. IEEE Access, **2023**, 11, pp.69884-69902.
21. Murmu, A. and Kumar, P., A novel Gateaux derivative with efficient DCNN-Resunet method for segmenting multi-class brain tumor. Medical & Biological Engineering & Computing, **2023**, 61(8), pp.2115-2138.
22. Tehsin, S., Nasir, I.M., Damaševičius, R. and Maskeliunas, R., DaSAM: Disease and spatial attention module-based explainable model for brain tumor detection. Big Data and Cognitive Computing, **2024**, 8(9), p.97.
23. Khan, M.S.I., Rahman, A., Debnath, T., Karim, M.R., Nasir, M.K., Band, S.S., Mosavi, A. and Dehzangi, I., Accurate brain tumor detection using deep convolutional neural network. Computational and structural biotechnology journal, **2022**, 20, pp.4733-4745.
24. Shaik, N.S. and Cherukuri, T.K., Multi-level attention network: application to brain tumor classification. Signal, Image and Video Processing, **2022**, 16(3), pp.817-824.
25. Nawaz, M. and Nazir, T., EDet-BTR: EfficientDet-based brain tumor recognition from the magnetic resonance imaging. Biomedical Signal Processing and Control, **2024**, 96, p.106618.
26. Treece, G., Real image denoising with a locally-adaptive bitonic filter. IEEE Transactions on Image Processing,**2022**, 31, pp.3151-3165.
27. Liu, J., Kang, H., Tao, W., Li, H., He, D., Ma, L., Tang, H., Wu, S., Yang, K. and Li, X., A spatial distribution–Principal component analysis (SD-PCA) model to assess pollution of heavy metals in soil. Science of The Total Environment, **2023**, 859, p.160112.
28. Charton, F., 2021. Linear algebra with transformers, 2024, arXiv preprint arXiv:2112.01898.
29. Kundu, S. and Kondor, R., Steerable transformers, **2024**,arXiv preprint arXiv:2405.15932.